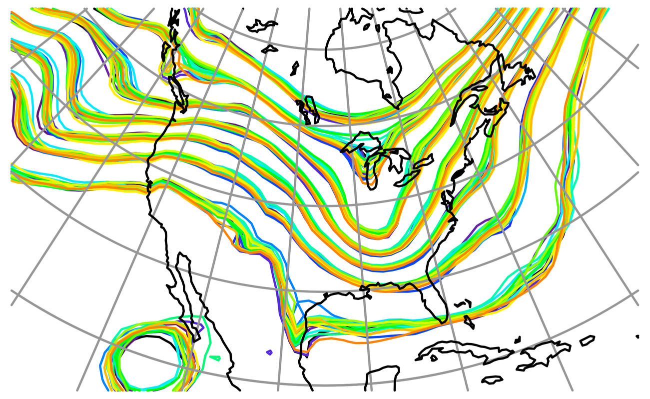

Improving Forecasts of Tropical Cyclones with Innovative GPSRO Satellite Observations

H. Liu, J. Anderson, Y.-H. Kuo, Y. Chen, and C. Snyder

National Center for Atmospheric Research
Institute for Mathematics Applied to Geosciences
Boulder, Colorado, USA
hliu@ucar.edu

1. Typhoon Shanshan (2006)

The tropical cyclone formed as a tropical depression on September 9, 2006 near 14N, 139E. It went through rapid intensification becoming a Category 4 storm by 12 September, 2006. It then moved northwestward and skirted to the east of Taiwan on 15 and 16 September, 2006. It was a challenge to predict the turning of the storm. The typhoon brought heavy rainfall over Taiwan and Eastern China.

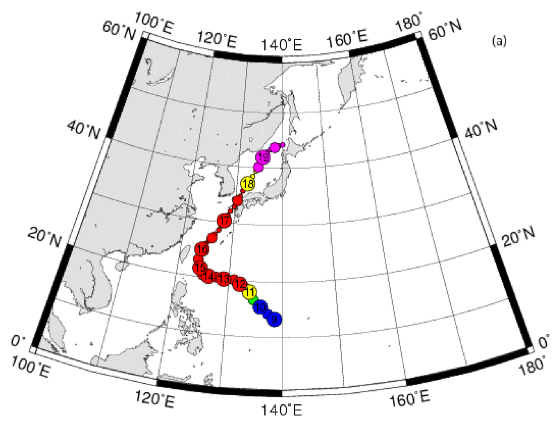

Figure 1: *Observed Best Track and intensity of Typhoon Shanshan (2006).*

2. GPS Radio Occultation (RO) Refractivity observations

2.1 What is GPS RO refractivity?

When radio signals from GPS satellites pass through the atmosphere, the raypaths are bent and the signal is slowed. The changes depend on the atmosphere's density along the path. Low-Earth-orbiting (LEO) satellites intercept the signals just above Earth's horizon and measure the bend and signal delay. The profiles of atmospheric refractivity as a function of height can be derived.

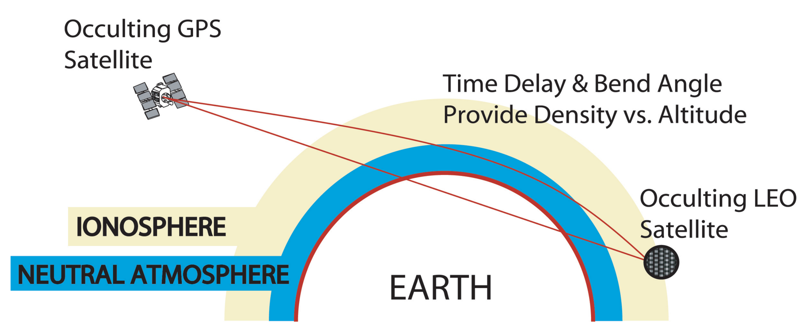

Figure 2: *Illustration of Radio Occultation.*

2.2 Reasons to use RO refractivity:

- only source of high vertical resolution (~200m near the surface) observations of water vapor for the middle and lower troposphere,
- provides large-scale observations of water vapor,
- is collected under all weather conditions.

2.3 Data availability

There were 24 GPS RO refractivity profiles available over the Western Pacific domain for 13 September 2006. These observations provided large-scale water vapor information.

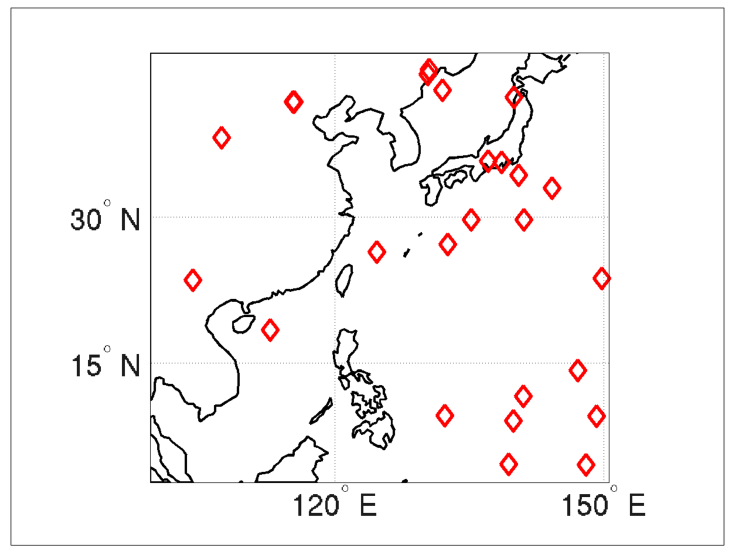

Figure 3: Locations of RO profiles over the Western Pacific domain, 13 September 2006.

3. Assimilation Experiments

3.1 WRF/DART Ensemble Assimilation System

NCAR's Weather and Research Forecast (WRF) model is a state-of-the-art mesoscale atmospheric model. The NCAR DART (Data Assimilation Research Testbed) ensemble data assimilation system was used to assimilate the observations into WRF, which was then run in forecast mode. This ensemble-based system is particularly good for mesoscale analysis because weather-dependent (i.e. spatially- and temporally-varying) forecast error covariances are used in the generation of the analyses.

3.2 Experiment Overview

Assimilations were done every 6 hours for September 13, 2006 and resulted in a final analysis at 00Z 14 September 2006. WRF was configured to run with 35 vertical levels at 36km horizontal resolution with a 120 second timestep. Thirty-two (32) ensemble members were used for the ensemble assimilation. Each ensemble member was then run forward to produce a 48-hour forecast. Two sets of nearly identical observations were used to determine the impact of the RO refractivity observations.

3.3 Experiment 'NOGPS'

The following observations were assimilated:

- Radiosonde temperature, moisture, and wind vectors (T,Q,U,V),
- Aircraft temperature and wind vectors (T,U,V),
- QuikSCAT ocean surface wind vectors (U,V), and
- Satellite cloud drift winds (U,V).

3.4 Experiment 'GPS'

The same observations as NOGPS as well as the RO refractivity observations from the COSMIC satellite network.

4. Results

4.1 Impact on track forecast

The left panel of Figure 4 depicts the performance of the 'NOGPS' experiment. The Best Track is not in the center of the tracks from the ensemble members. The panel on the right is the result of the 'GPS' experiment. The ensemble tracks are more symmetrically distributed around the Best Track and result in an ensemble mean that is much more representative of the Best Track. With the GPS RO observations, the ensemble performs better, especially at the later stage of the forecasts. As the storm matures, the vortex center is more reliably estimated.

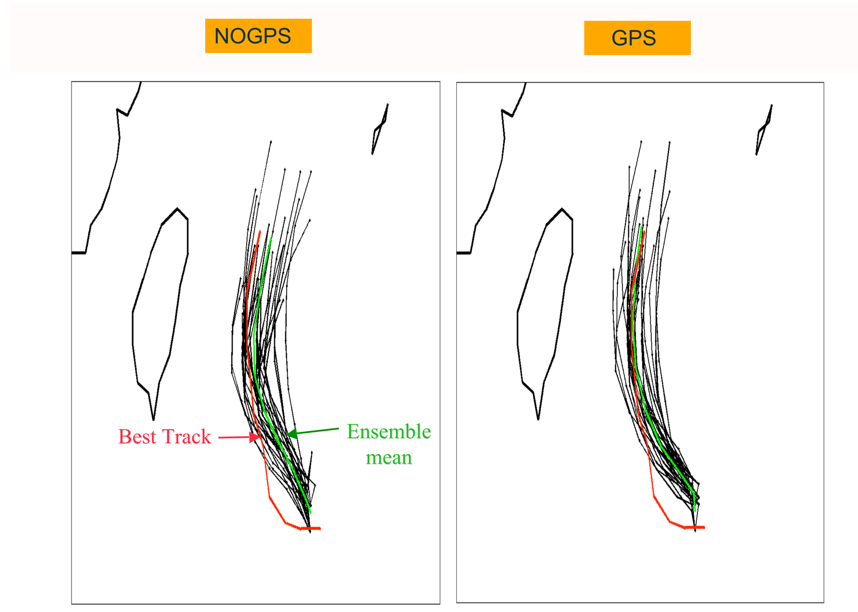

Figure 4: *Track forecasts for both experiments. The start of the tracks is at 14 Sep 00Z (the end of the data assimilation period) and ends at 16 Sep 00Z. The position of the vortex center for each ensemble member forecast is depicted as a thin black line. The (observed) Best Track is shown in red, the average of the ensemble is shown in green.*

4.2 Impact on intensity forecast

The intensity of the typhoon's minimum central sea level pressure is also enhanced (by several hPa) by assimilating the GPS RO observations. The 36km grid size is fundamentally too coarse to accurately represent the storm intensity.

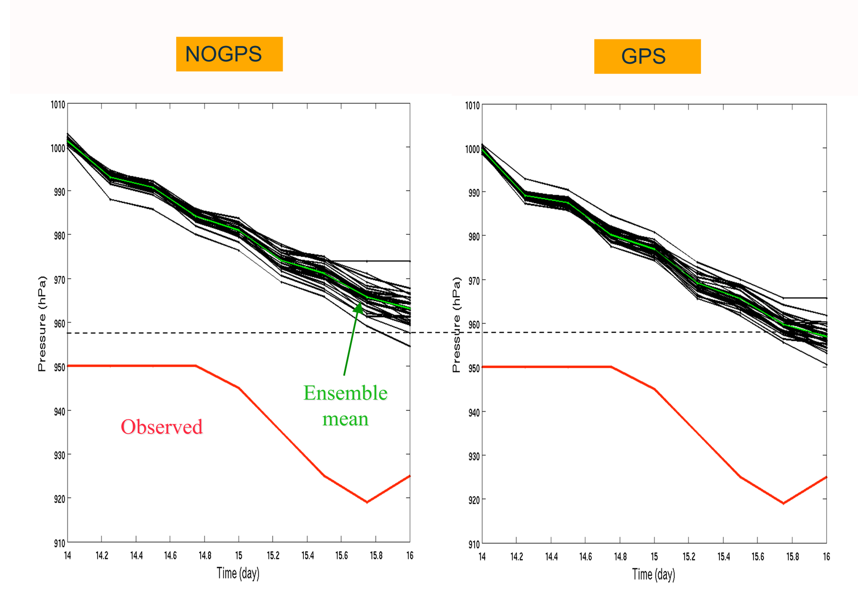

Figure 5: *Ensemble forecasts of the central minimum sea level pressure for 14 Sep 00Z through 16 Sep 00Z for both experiments. The assimilations using the GPS RO observations result in a slight improvement in intensity.*

4.3 Impact on precipitation forecast

The GPS experiment forecasts of probability of heavy precipitation over Taiwan more closely match the heavy precipitation that was observed. In general, the GPS experiment forecasts have a higher probability of heavy precipitation.

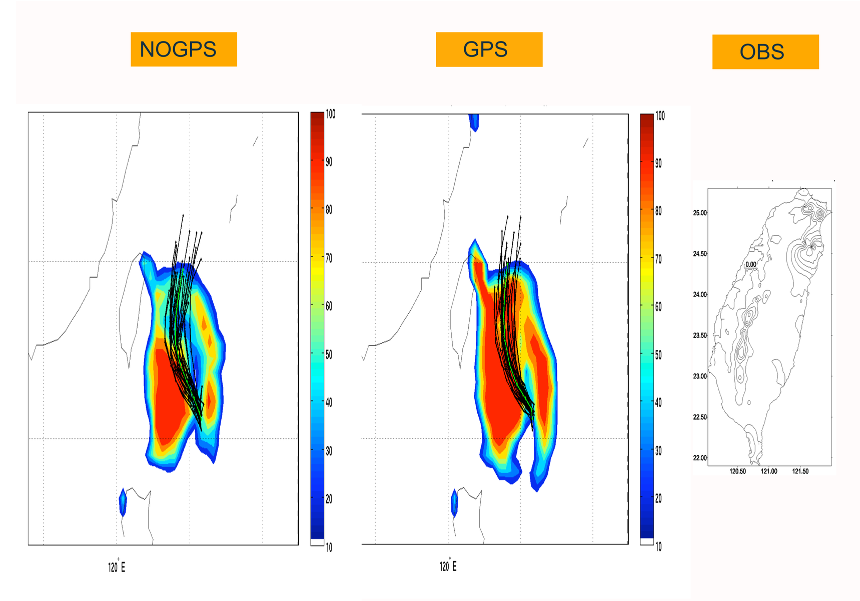

Figure 6: *The two panels on the left show the probability forecast of 24-hour accumulated rainfall $>$ 60mm/day during the 24-hour period starting 12Z 14 Aug 2006. Note: the panel on the right (showing the observed rainfall) is not to scale with the other two panels in an attempt to highlight the rainfall amounts over northern Taiwan.*

5. Conclusion

It can be concluded the GPS RO observations improved the ensemble forecasts of the Typhoon Shanshan. More cases are being studied to evaluate the impact of this new type of satellite observations.

6. For further information

Our DART web site is: **http://www.image.ucar.edu/DAReS/DART** There you will find information about how to download the latest revision of DART from our subversion server, information on a full DART tutorial (included with the distribution), and contact information for the DART development group.

References

[1] R.A. Anthes et.al., 2008: The COSMIC/FORMOSAT-3 Mission: Early Results *BAMS*, **89** No. 3 pp. 313–333